

Rheology of bidisperse non-Brownian suspensions

Abhinendra Singh,^{1,2,3,*} Christopher Ness,⁴ Abhishek K. Sharma,³ Juan J de Pablo,^{3,5} and Heinrich M Jaeger^{2,6}

¹*Department of Macromolecular Science and Engineering,
Case Western Reserve University, Cleveland, OH, 10040, USA*

²*James Franck Institute, University of Chicago, Chicago, Illinois 60637, USA*

³*Pritzker School of Molecular Engineering, University of Chicago, Chicago, Illinois 60637, USA*

⁴*School of Engineering, University of Edinburgh, Edinburgh EH9 3FG, United Kingdom*

⁵*Materials Science Division, Argonne National Laboratory, Lemont, Illinois 60439, USA*

⁶*Department of Physics, The University of Chicago, Chicago, Illinois 60637, USA*

(Dated: November 13, 2023)

We study the rheology of bidisperse non-Brownian suspensions using particle-based simulation, mapping the viscosity as a function of the size ratio of the species, their relative abundance, and the overall solid content. The variation of the viscosity with applied stress exhibits paradigmatic shear thickening phenomenology irrespective of composition, though the stress-dependent limiting solids fraction governing the viscosity and its divergence point are non-monotonic in the mixing ratio. Contact force data demonstrate an exchange in dominant stress contribution from large-large to small-small particle contacts as the mixing ratio of the species evolves. Combining a prior model for shear thickening with one for composition-dependent jamming, we obtain a full description of the rheology of bidisperse non-Brownian suspensions capable of predicting effects such as the viscosity reduction observed upon adding small particle fines to a suspension of large particles.

Introduction. Suspensions of small particles, radius $a \approx 100 \text{ nm} - 10 \text{ }\mu\text{m}$, form a class of complex fluids abundant in nature and industry [1–3]. Their widespread use calls for detailed constitutive characterization to enable reliable process design [4], especially in the dense regime where particles and fluid are mixed roughly equally [5]. Under external deformation, these systems, which are apparently simple in composition, exhibit complex rheology including yielding, shear thinning, shear thickening, and jamming [5–7]. Recently this phenomenology has been linked to microscopic physics, specifically constraints that control the relative translation and rotation of interacting particle pairs [8–10]. Shear thickening, for example, represents a crossover from unconstrained to constrained tangential motion as the imposed particle stress σ exceeds a threshold set by the repulsive force $\sigma_0 \sim F_0/a^2$ [11]. A mean-field approach by Wyart and Cates [12] (WC) captures the transition using stress-dependent jamming volume fraction $\phi_J(\sigma)$ interpolating between low (ϕ_0) and high (ϕ_m) stress limits, reproducing (in some cases quantitatively) the steady state rheology [8, 13].

The above conceptual framework was devised based on nearly monodisperse suspensions, and most numerical and experimental works that seek to test it reflect this [13–17]. As soon as significant deviations from monodispersity are considered, however, complexity emerges that is not captured by WC. In particular, adding small particles to a system of large ones can reduce the viscosity under shear [4, 18, 19], yet in the reverse case when larger particles are added to small ones, only an increase in viscosity is reported [20–22]. Extending the understanding of constraint-controlled rheology to suspensions with size-disperse particles is thus a key open problem. Our approach addresses this challenge

in a model system of just two species. Already in this minimal system, particle size disparity can have a profound effect on the rheology, which, with the exception of a few recent works [16, 23–25], has remained largely unexplored.

The rheology of bidisperse suspensions is governed by ϕ_J , which is controlled by the species size ratio Δ , their volumetric mixing ratio $\alpha = N_S a_S^3 / (N_S a_S^3 + N_L a_L^3)$, and the particle friction coefficient μ [26]. Previous experimental [26, 27] and numerical [16, 23, 24] studies show that for a constant solids fraction ϕ , the relative suspension viscosity η_r decreases with Δ at fixed α while varying non-monotonically with α at fixed Δ . This was explained on the basis of ϕ_J being non-monotonic in α , for which several models have been proposed [28, 29]. In dry granular materials it is understood that ϕ_J depends on (Δ, α, μ) [30], and there have been attempts to relate this to the fraction of smaller particles being rattlers [30, 31].

In this Letter, we explore systematically the role of bidispersity on the rheology of dense, non-Brownian suspensions using an established simulation scheme [11, 32]. We explore $\Delta \leq 12$, $0 < \alpha < 1$ and ϕ close to the jamming point. We show that the non-monotonic $\eta_r(\alpha)$ coincides with an exchange of stress contribution dominance from large-large (LL) contacts at small α to small-small (SS) contacts at large α , while the stress carried by large-small (LS) contacts is non-monotonic in α and vanishes at the extremes. Combining an *ad hoc* extension of WC with a geometric model for $\phi_J(\Delta, \alpha)$ by Yu and Standish [28] (YS), we obtain qualitative predictions of the rheology for any bidisperse, shear thickening, non-Brownian suspension. Using the model, we explore practical settings where small additives are incorporated into suspensions of large particles, rationalising the counter-intuitive

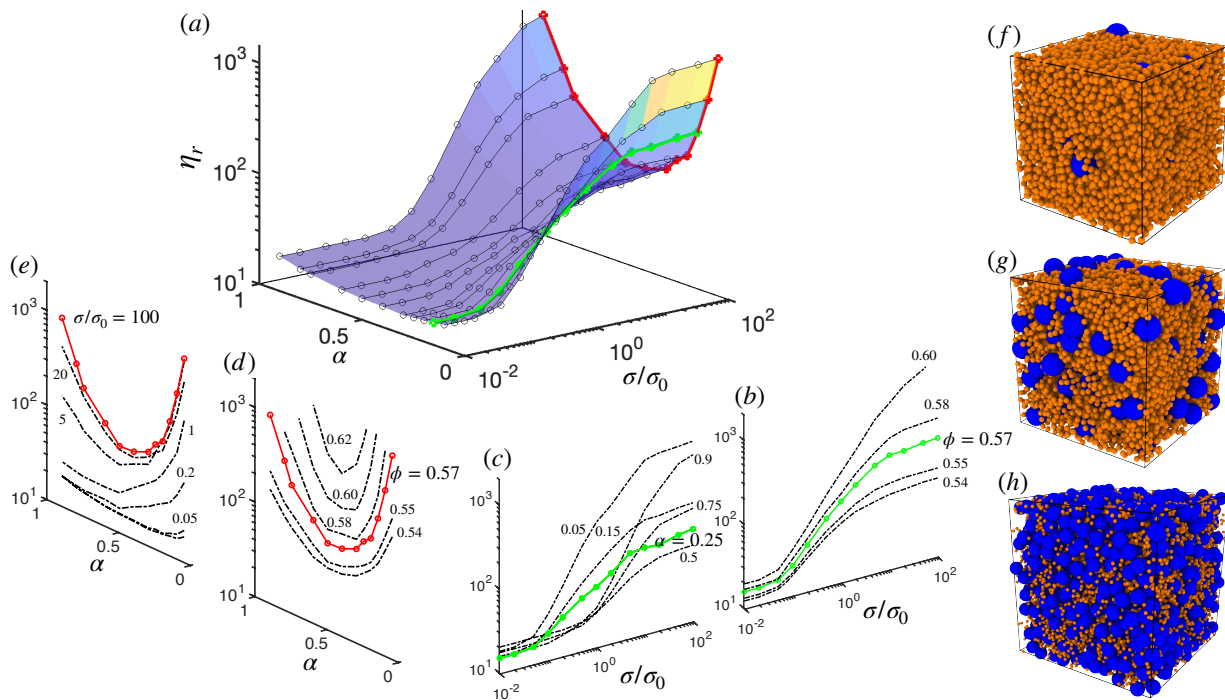


FIG. 1. Effect of mixing small and large particles on the rheology of a model suspension with size ratio $\Delta = 4$. Shown are (a) the relative viscosity η_r as a function of the volume ratio of small particles α and the applied stress σ/σ_0 , at $\phi = 0.57$. Red and green lines represent common data sets across each panel, showing, respectively, $\eta_r(\alpha)$ for $\sigma/\sigma_0 = 100$, and $\eta_r(\sigma)$ for $\alpha = 0.25$. (b) η_r as a function of σ/σ_0 at fixed $\alpha = 0.25$ for various ϕ . (c) η_r as a function of σ/σ_0 at fixed $\phi = 0.57$ for various α . (d) η_r as a function of α for various ϕ at fixed $\sigma/\sigma_0 = 100$ (e) η_r as a function of α for $\phi = 0.57$ for various σ/σ_0 . (f)-(h) Snapshots of the simulation at $\phi = 0.57$, $\sigma/\sigma_0 = 100$, $\Delta = 4$, and (top-to-bottom) $\alpha = 0.9, 0.5, 0.1$.

finding that increasing ϕ can in some circumstances reduce η_r . Meanwhile adding large particles to a suspension of small ones always enhances η_r , corroborating experimental findings [21, 22].

Simulations. We model 6000 spheres for $\Delta \leq 6$ (12000 for $\Delta = 12$) dispersed in density-matched Newtonian liquid under imposed shear stress σ , in a constant volume periodic domain. The suspension flows with time-dependent shear rate $\dot{\gamma}(t)$, and we compute the relative viscosity as $\eta_r(t) = \sigma/\eta\dot{\gamma}(t)$, with η the liquid viscosity. Rheology data shown in the following are averages of η_r over 5 strain units at steady state, across 5 realizations. Particles interact through short-range hydrodynamic lubrication and contact forces and torques. The latter includes a tangential component regulated by a sliding friction coefficient $\mu = 1$ (with rolling friction [9] absent), activated above a threshold normal force F_0 [11, 33] giving a characteristic stress scale $\sigma_0 = F_0/a^2$. We perform simulations for $\Delta = 2, 3, 4, 6, 12$ and $\alpha = [0.05, 0.9]$.

Bidisperse suspension rheology. Figure 1 shows the effect of α on the rheology for exemplar data with $\Delta = 4$. We present a map of (η_r, α, σ) at $\phi = 0.57$ in Fig. 1(a) showing an overview of the behavior, with planar slices showing (b) $\eta_r(\sigma/\sigma_0, \phi)$ at $\alpha = 0.25$; (c) $\eta_r(\sigma/\sigma_0, \alpha)$ at $\phi = 0.57$; (d) $\eta_r(\alpha, \phi)$ at $\sigma/\sigma_0 = 100$; (e) $\eta_r(\alpha, \sigma/\sigma_0)$ at $\phi = 0.57$. In Figs. 1(f)-(h) are snapshots of the simula-

tion at $\alpha = 0.9, 0.5, 0.1$. In Fig 1(b), one observes canonical thickening behavior, qualitatively similar to quasis-monodisperse systems showing a stress-mediated transition between two Newtonian plateaus [14, 15, 33]. The viscosities of the plateaus increase with ϕ towards their respective jamming points $\phi_0 \equiv \phi_J(\sigma/\sigma_0 \rightarrow 0) \approx 0.75$ and $\phi_m \equiv \phi_J(\sigma/\sigma_0 \rightarrow \infty) \approx 0.65$ (these numbers being sensitive to α , Δ and μ). In Fig. 1(c) we find that σ_0 increases monotonically with α (since the former is related to the particle size through $\sigma_0 \sim F_0/a^2$), while the frictionless and frictional viscosities measured at $\sigma/\sigma_0 = 0.01$ and $\sigma/\sigma_0 = 100$ respectively show non-monotonic dependence on α . The crossover of these flow curves is a result of the combined effect of bidispersity on σ_0 and ϕ_J and is not predicted by models that assume monodispersity. Next we present data in the $\eta_r(\alpha)$ plane. Figure 1(d) shows η_r for $\sigma/\sigma_0 = 100$ as a function of α for various ϕ . At fixed ϕ , η_r first decreases with increasing α , reaching a minimum before increasing again so that $\eta_r(\alpha = 0) = \eta_r(\alpha = 1)$. In the limits $\alpha = (0, 1)$ the suspension is monodisperse and exhibits identical rheology due to the size invariance of non-Brownian suspensions (when σ/σ_0 is 0 or ∞). The value of α that minimizes η_r is insensitive to ϕ . For $\phi \geq 0.58$, the suspension near the extrema $\alpha = 0, 1$ is jammed, and the window of α for which η_r is finite decreases with increasing ϕ so that

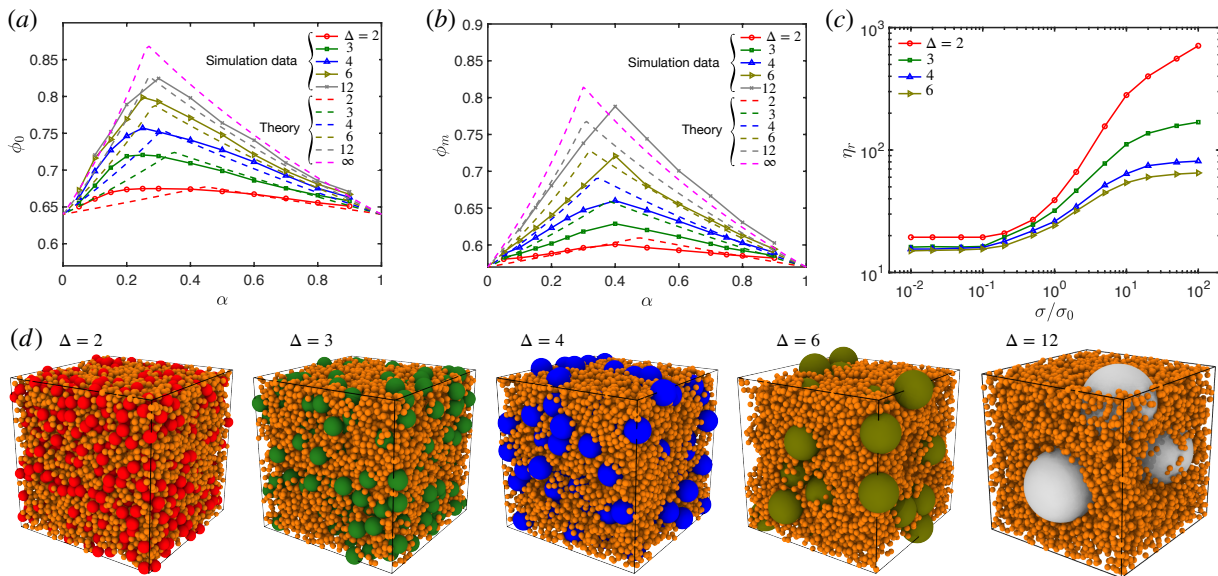


FIG. 2. Role of the particle size ratio Δ . (a) Variation with α of ϕ_0 , the jamming point at $\sigma/\sigma_0 = 0$, for a range of Δ . Solid lines with points represent simulation data; dashed lines show model predictions [28]; (b) Variation with α of ϕ_m , the jamming point at $\sigma/\sigma_0 = \infty$, for a range of Δ ; (c) Relative viscosity η_r as a function of σ/σ_0 at $\phi = 0.57$ and $\alpha = 0.5$ for various Δ . (d)-(f) Snapshots of simulations with $\phi = 0.5$, $\mu = 1$, $\alpha = 0.5$ and (left to right) $\Delta = 2, 3, 4, 6, 12$.

no flow occurs at any α for $\phi \geq 0.65$. Figure 1(e) shows $\eta_r(\alpha)$ for various σ/σ_0 at fixed $\phi = 0.57$. For $\sigma/\sigma_0 = 100$, η_r at the large and small limits of α are equal, while for $\sigma/\sigma_0 \leq 5$, η_r is higher for small α ($\alpha \rightarrow 0$) as compared to larger values ($\alpha \rightarrow 1$). This can be explained based on the relation between σ_0 and particle size a . Since $\sigma_0 \sim 1/a^2$, σ_0 increases with α (Fig. 1(c)) so that the jamming point is governed by friction at lower stress when particles are large.

Figure 2 shows the effect of Δ on the jamming points ϕ_0 , ϕ_m , and on η_r . In Figs. 2(a) and (b) are the variation of ϕ_0 and ϕ_m with α , for $\Delta = (2, 3, 4, 6, 12)$, obtained by simulating the limits $\sigma/\sigma_0 \rightarrow 0$ and $\sigma/\sigma_0 \rightarrow \infty$ for a range of ϕ , then fitting the viscosity as $\eta_r = (1 - \phi/\phi_{m,0})^{-2}$ [34]. Both ϕ_0 and ϕ_m vary non-monotonically with α , with the dependence being more pronounced for increasing Δ . Also plotted are $\phi_{0,m}$ predictions as functions of α at various Δ following the model of Yu and Standish [28], which produces jamming point predictions based on geometry only. Interestingly the model works better for the frictionless limit (ϕ_0 , $\sigma/\sigma_0 = 0$) as compared to the frictional one (ϕ_m , $\sigma/\sigma_0 = \infty$), likely due to the absence of friction and shear-induced structure in the theory. (Indeed, understanding the disparity in the nature of jamming between frictionless and frictional systems remains an open challenge [35].) In the frictionless case, the simulation data appear to be converging toward the theory, though testing this for larger Δ rapidly becomes computationally intractable. Plotting η_r as a function of σ/σ_0 for different Δ at fixed $\alpha = 0.5$, $\phi = 0.57$ (Fig. 2(c)), one finds the viscosity of both limiting states

decreases with increasing Δ , as the proximity to jamming is decreased.

Contribution of different contact types. We next address the microscopic underpinning of the non-monotonic $\eta_r(\alpha)$ reported in Fig. 1 (see also [23, 24, 26]), using simulation data to separate the stress contributions of different types of contacts LL, LS, and SS. Figure 3(a) shows the viscosity contribution of each contact type scaled

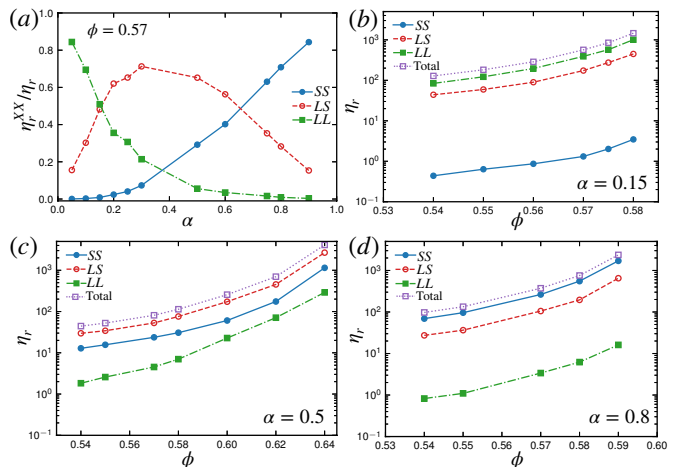


FIG. 3. Viscosity contributions from each contact type. (a) Relative contribution η_r^{XX} to the total viscosity η_r of each contact type (where SS, LS, and LL replace XX) as a function of α , for $\phi = 0.57$ and $\sigma/\sigma_0 = 100$; (b)-(d) Total viscosity and its contact contributions as a function of ϕ at $\sigma/\sigma_0 = 100$ for $\alpha =$ (b) 0.15; (c) 0.5, and (d) 0.8;

with η_r for $\phi = 0.57$ at $\sigma/\sigma_0 = 100$ as a function of α for $\Delta = 4$. At small α , LL contacts provide the dominant contribution to η_r , while SS take over at large α as expected. LL decay from 1 at $\alpha = 0$ (by definition) to ≈ 0 for $\alpha \geq 0.6$ with the SS contribution being minimal for $\alpha \leq 0.2$ and increasing to 1 at $\alpha = 1$. Notably the value of α at which SS contributions begin to increase and LL vanishes are not symmetric with respect to 0 and 1, and the contribution of LS is non-monotonic: by definition it vanishes for $\alpha = 0, 1$, and is maximal around $\alpha = 0.4$ where it contributes $\approx 75\%$ of the overall viscosity. Generalizing these findings for different values of ϕ , Figs. 3(b)-(d) present η_r as a function of ϕ for $\alpha = 0.15, 0.5$, and 0.8 respectively, demonstrating that LL and SS are the dominant contributors to jamming at $\alpha = 0.15$ and 0.8 , respectively, while for $\alpha = 0.5$ the major contribution to originates from LS.

Constitutive model. Given the qualitative agreement of the dependence of ϕ_0 and ϕ_m on α and Δ with YS and of $\eta_r(\sigma/\sigma_0)$ with WC, we are motivated to construct a combined model to capture the full behavior. Conventional WC writes $\eta_r(\sigma/\sigma_0) = (1 - \phi/\phi_J(\sigma/\sigma_0))^{-2}$ with $\phi_J(\sigma/\sigma_0) = f\phi_m + (1 - f)\phi_0$ and $f = \exp(-\sigma/\sigma_0)$. Here we let ϕ_0 and ϕ_m be functions of α and Δ as plotted in Fig. 2(a)-(b), and we let σ_0 interpolate in an *ad hoc* way between small and large particle limits as $\sigma_0 = F_0/(\alpha a_S + (1 - \alpha)a_L)^2$. Doing so one obtains a qualitative picture of the rheology, Fig. 4(a).

Using this model we can predict the effect on the rheology of compositional changes. To demonstrate this, we consider in Fig. 4(b)-(d) the effect of adding small particles to a suspension of monodisperse large ones, for $\sigma/\sigma_0 = \infty$ and $\Delta = 4$. Counter-intuitively, for sufficiently large initial ϕ (of large particles), the addition of small particles leads to a decrease in η_r . The model predicts that the increase in ϕ is slower than that of ϕ_m , hence $(1 - \phi/\phi_m)^{-2}$ decreases. Conversely, the asymmetry in $\phi_m(\alpha)$ means adding large particles to a packing of small ones leads, more intuitively, to an increase in both ϕ and η_r (Fig. 4(e)-(g)). At intermediate σ/σ_0 , ϕ_J interpolates between frictionless and frictional values (Fig. 4(h)), and the range of α for which viscosity reduction appears is broadened (Fig. 4(i)-(j)). Recent experiments have shown that adding large non-Brownian particles to a suspension of small ones leads to enhanced thickening behavior [21, 22], consistent with our prediction (Fig. 4(e)) that doing so will always move the system closer to its respective ϕ_m .

Concluding remarks. We have shown that an existing constitutive relation for rate-dependent rheology (WC, [12]) can be combined in an *ad hoc* way with a geometric model by Yu and Standish [28] to obtain a qualitative picture of the rheology of bidisperse suspensions. Our ansatz for $\sigma_0(\alpha)$ is not strictly in accordance with WC, in the sense that the order parameter f can no longer represent the fraction of contacts that are fric-

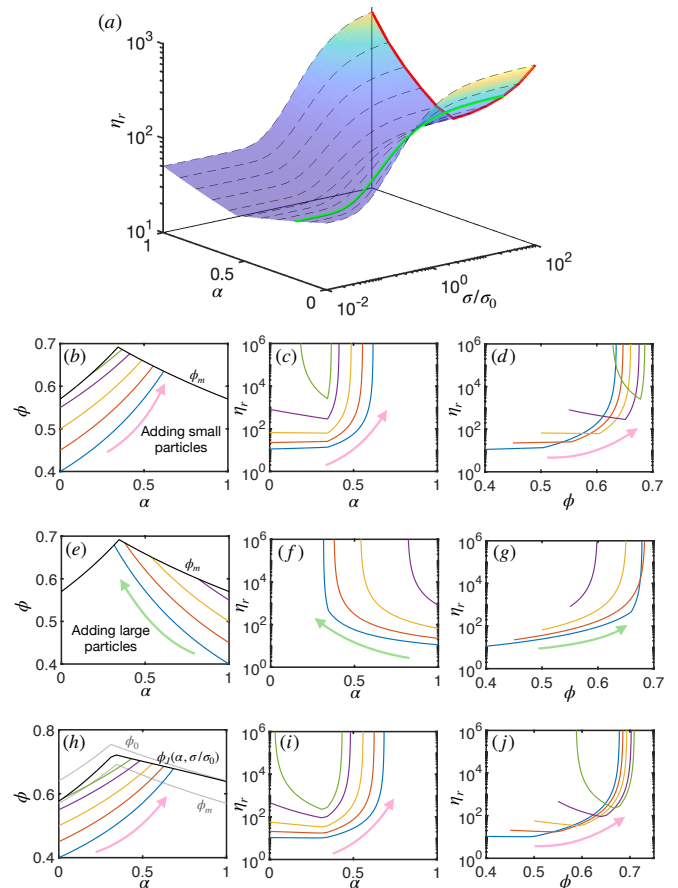


FIG. 4. Constitutive model predictions. (a) Combining the WC model for $\eta_r(\sigma/\sigma_0)$ with the YS model for $\phi_J(\alpha, \Delta)$, one obtains the rheology of bidisperse frictional suspensions. (b)-(d) Adding small particles to a monodisperse large particle packing at $\sigma/\sigma_0 = \infty$: (b) Variation of ϕ and ϕ_m with α , and η_r plotted as a function of (c) α and (d) ϕ . (e)-(g) Adding large particles to a monodisperse small particle packing at $\sigma/\sigma_0 = \infty$: (e) Variation of ϕ and ϕ_m with α , and η_r plotted as a function of (f) α and (g) ϕ . (h)-(i) Adding small particles to a monodisperse large particle packing at intermediate σ/σ_0 , so that large particles are frictional and small ones are frictionless. (h) Variation of ϕ and ϕ_J with α , and η_r plotted as a function of (i) α and (j) ϕ . Also shown in (h) in gray are ϕ_m and ϕ_0 . Colors in (b)-(j) represent different initial ϕ ; black lines represent $\phi_m(\alpha)$ and $\phi_J(\alpha, \sigma/\sigma_0)$. Colored arrows indicate adding small (pink) and large (green) particles.

tional (see Ref [16] for more details). Nonetheless our model predicts novelty in the rheology that is present in reality but unaddressed by WC, specifically that adding small particles to a system of large ones can counterintuitively decrease the viscosity, whereas in the opposite case adding large particles to small particles always leads to an increase in η_r . We show additionally that the non-monotonic dependence of relative viscosity η_r on α for constant ϕ (as reported by [23, 24, 26, 27]) can be understood by delineating the stress contributions of each type of contact, and our results suggest that the rheol-

ogy at $\Delta = 12$ is already close to the $\Delta \rightarrow \infty$ limit, so the predictions made here will be useful across bidisperse systems of arbitrary size ratio. The consequences of these results for more complex systems, especially polydisperse samples [36] in which colloidal forces may become relevant [37], are broad. In particular, our results provide a direction towards the limiting case of predicting the rheology of mixtures where larger additives are included in a continuous background phase of much smaller particles [20]. Although we have focused on the model systems of two species, the results can be used to qualitatively predict the rheology of polydisperse suspensions, which has many applications: industrial processing of slurries and muds; manufacturing of amorphous solid dispersions; and predicting the runout of geophysical flows comprising grains spanning many orders of magnitude [38].

Codes and scripts necessary to reproduce the results reported in this article are available on request. We acknowledge support from the Center for Hierarchical Materials Design (CHiMaD) under award number 70NANB19H005 (US Dept. Commerce), and from the Army Research Office under grants W911NF-19-1-0245, W911NF-21-2-0146, and W911NF-21-1-0038. A. S. acknowledges Case Western Reserve University for start-up funding. C.N. thanks Eric Breard for pointing to Ref [28], and acknowledges support from the Royal Academy of Engineering under the Research Fellowship scheme and from the Leverhulme Trust under Research Project Grant RPG-2022-095. Part of this work made use of the High Performance Computing Resource in the Core Facility for Advanced Research Computing at Case Western Reserve University.

A.S. and C.N. contributed equally to this work.

* abhinendra.singh@case.edu

- [1] C. Ness, R. Seto, and R. Mari, *Annual Review of Condensed Matter Physics* **13**, 97 (2022).
- [2] J. F. Morris, *Annual Review of Fluid Mechanics* **52**, 121 (2020).
- [3] A. Singh, *MRS Communications*, 1 (2023).
- [4] N. Roussel, A. Lemaître, R. J. Flatt, and P. Coussot, *Cement and Concrete Research* **40**, 77 (2010).
- [5] E. Brown and H. M. Jaeger, *Reports on Progress in Physics* **77**, 046602 (2014).
- [6] I. R. Peters, S. Majumdar, and H. M. Jaeger, *Nature* **532**, 214 (2016).
- [7] A. Singh, S. Pednekar, J. Chun, M. M. Denn, and J. F. Morris, *Physical Review Letters* **122**, 098004 (2019).
- [8] B. M. Guy, J. Richards, D. Hodgson, E. Blanco, and W. C. K. Poon, *Physical Review Letters* **121**, 128001 (2018).
- [9] A. Singh, C. Ness, R. Seto, J. J. de Pablo, and H. M. Jaeger, *Physical Review Letters* **124**, 248005 (2020).
- [10] A. Singh, G. L. Jackson, M. van der Naald, J. J. de Pablo, and H. M. Jaeger, *Physical Review Fluids* **7**, 054302 (2022).
- [11] R. Seto, R. Mari, J. F. Morris, and M. M. Denn, *Physical Review Letters* **111**, 218301 (2013).
- [12] M. Wyart and M. E. Cates, *Physical Review Letters* **112**, 098302 (2014).
- [13] A. Singh, R. Mari, M. M. Denn, and J. F. Morris, *Journal of Rheology* **62**, 457 (2018).
- [14] B. M. Guy, M. Hermes, and W. C. K. Poon, *Physical Review Letters* **115**, 088304 (2015).
- [15] C. Ness and J. Sun, *Soft Matter* **12**, 914 (2016).
- [16] B. M. Guy, C. Ness, M. Hermes, L. J. Sawiak, J. Sun, and W. C. Poon, *Soft Matter* **16**, 229 (2020).
- [17] S. Pradeep, M. Nabizadeh, A. R. Jacob, S. Jamali, and L. C. Hsiao, *Physical Review Letters* **127**, 158002 (2021).
- [18] H. Van Damme, *Cement and Concrete Research* **112**, 5 (2018).
- [19] R. Flatt, *Materials and Structures* **37**, 289 (2004).
- [20] C. D. Cwalina and N. J. Wagner, *Journal of Rheology* **60**, 47 (2016).
- [21] Y. Madraki, S. Hormozi, G. Ovarlez, E. Guazzelli, and O. Pouliquen, *Physical Review Fluids* **2**, 033301 (2017).
- [22] Y. Madraki, G. Ovarlez, and S. Hormozi, *Physical Review Letters* **121**, 108001 (2018).
- [23] N. Malbranche, B. Chakraborty, and J. F. Morris, *Journal of Rheology* **67**, 91 (2023).
- [24] S. Pednekar, J. Chun, and J. F. Morris, *Journal of Rheology* **62**, 513 (2018).
- [25] A. Monti and M. E. Rosti, *Meccanica* **58**, 727 (2023).
- [26] B. J. Maranzano and N. J. Wagner, *Journal of Chemical Physics* **114**, 10514 (2001).
- [27] B. J. Maranzano and N. J. Wagner, *Journal of Rheology* **45**, 1205 (2001).
- [28] A.-B. Yu and N. Standish, *Industrial & Engineering Chemistry Research* **30**, 1372 (1991).
- [29] F. Qi and R. I. Tanner, *Korea-Australia Rheology Journal* **23**, 105 (2011).
- [30] I. Srivastava, S. A. Roberts, J. T. Clemmer, L. E. Silbert, J. B. Lechman, and G. S. Grest, *Physical Review Research* **3**, L032042 (2021).
- [31] J. C. Petit, N. Kumar, S. Luding, and M. Sperl, *Physical Review Letters* **125**, 215501 (2020).
- [32] R. Mari, R. Seto, J. F. Morris, and M. M. Denn, *Physical Review E* **91**, 052302 (2015).
- [33] R. Mari, R. Seto, J. F. Morris, and M. M. Denn, *Journal of Rheology* **58**, 1693 (2014).
- [34] I. M. Krieger and T. J. Dougherty, *Transactions of the Society of Rheology* **3**, 137 (1959).
- [35] A. J. Liu and S. R. Nagel, *Annual Review of Condensed Matter Physics* **1**, 347 (2010).
- [36] P. M. Mwasame, N. J. Wagner, and A. N. Beris, *Journal of Rheology* **60**, 225 (2016).
- [37] X. Li, J. R. Royer, and C. Ness, arXiv preprint arXiv:2307.13802 (2023).
- [38] E. C. Breard, J. Dufek, S. Charbonnier, V. Gueugneau, T. Giachetti, and B. Walsh, *Nature Communications* **14**, 2079 (2023).